Bulletin of the Seismological Society of America, Vol. 96, No. 2, pp. 586–598, April 2006, doi: 10.1785/0120050109

Extracting the Building Response Using Seismic Interferometry: Theory and Application to the Millikan Library in Pasadena, California

by Roel Snieder and Erdal Şafak

Abstract The motion of a building depends on the excitation, the coupling of the building to the ground, and the mechanical properties of the building. We separate the building response from the excitation and the ground coupling by deconvolving the motion recorded at different levels in the building and apply this to recordings of the motion in the Robert A. Millikan Library in Pasadena, California. This deconvolution allows for the separation of instrinsic attenuation and radiation damping. The waveforms obtained from deconvolution with the motion in the top floor show a superposition of one upgoing and one downgoing wave. The waveforms obtained by deconvolution with the motion in the basement can be formulated either as a sum of upgoing and downgoing waves, or as a sum over normal modes. Because these deconvolved waves for late time have a monochromatic character, they are most easily analyzed with normal-mode theory. For this building we estimate a shear velocity $c = 322$ m/sec and a quality factor $Q = 20$. These values explain both the propagating waves and the normal modes.

Introduction

The response of a building to natural or man-made shaking is largely determined by the velocity of shear waves and their attenuation in the building. The shear velocity, together with the geometry of the building, controls the resonant frequencies of the building. The attenuation determines the rate of energy dissipation in the building, which in turn controls the motion of the building for a given excitation.

A complicating factor in the response of a building to shaking is that this response depends both on the properties of the building and on the nature of the coupling to the subsurface (Şafak, 1995) and the associated radiation damping (Snieder, 2004b). It has been documented that the resonant frequencies of a building can change after heavy precipitation, which changes the coupling between the building and the ground with soil moisture (Clinton, 2004). The ground motion itself can also alter the coupling of a building to the subsurface (Trifunac *et al.*, 2001a, b). To fully understand the response of the building, one needs to unravel the properties of the building itself from the coupling of the building to the ground. This work is aimed at retrieving the building response from the recording of incoherent shaking of the building and to unravel the properties of the building itself from the coupling of the building to the subsurface.

We analyze this problem using a technique referred to as seismic interferometry. This technique is based on the correlation of waves recorded at different receivers. When the excitation of the waves is evenly distributed in space, or among the normal modes of the system, this correlation can be shown to lead to the Green's function that accounts for the wave propagation between receivers (Lobkis and Weaver, 2001; Derode *et al.*, 2003; Snieder, 2004a; Wapenaar, 2004; Snieder *et al.*, 2006). This technique is valuable because it enables the study of the waves that propagate between receivers without needing a source at one of the receiver locations. It does not matter whether the waves recorded at the receivers are excited by coherent sources or incoherent sources. Here we apply this technique to extract the building response of the Robert A. Millikan Library in Pasadena, California. In contrast to earlier work on seismic interferometry we base our analysis on the deconvolution of the recorded waves at different locations in the building rather than on the correlations.

In the next section we give details on the Robert A. Millikan Library and the employed recordings of the motion of the building. We describe the deconvolution that we use in the Deconvolved Waves section, and we show in the section Deconvolution Changes the Boundary Condition that the deconvolved waveforms satisfy a boundary condition at the base of the building different from the recorded waves. In the section Simple Model for the Wave Propagation in the Building we present a simple analytical model of the motion of the building that is based on interfering upgoing and downgoing waves. We show that the deconvolution gives a response that is independent of the excitation and that it does not depend on the coupling of the building with the ground. We show that these deconvolved waves can be

interpreted either as propagating waves or as normal modes. We use the deconvolved waves in the section Interpretation of the Deconvolved Waveforms to determine the shear velocity and the attenuation of the building. In the appendix we use integration in the complex plane to show how the normal modes of the building can be obtained from the deconvolved waveforms.

In this work we assume that the response of the building and the underlying soil is linear and time invariant. The linearity of the building response breaks down when strong shaking damages the building. Trifunac *et al.* (2001a,b) have shown that shaking at a moderate intensity may lead to changes in the dynamic properties of the soil and the building.

The Millikan Library and the Recorded Waves

The Robert A. Millikan Library is a ten-story reinforced-concrete building located on the campus of the California Institute of Technology in Pasadena, California. Completed in 1967, the building is 21 × 22.9 m in plan, and 43.9 m high from the ground level. The north–south elevation of the building, and the plans for a typical floor and the foundation are given in Figures 1 and 2, respectively. There is a 4.3-m-deep basement level below the ground. The structural system includes moment-resisting frames and shear walls. The shear walls at the center of the building form the elevator shaft and carry lateral loads in the east–west direction, whereas the curved shear walls at the east and west ends carry lateral loads in the north–south direction. The foundation system is composed of a central pad 32 feet wide by 4 feet deep that extends between the east and west curved shear walls. In addition, 10-feet-wide and 2-feet-deep continuous foundation beams run in the east–west direction beneath the columns at the north and south ends of the building. The alluvium under the foundation consists of medium to dense sands mixed with gravels to the bedrock at a distance of about 275 m. The water table is about 11 m deep (Kuroiwa, 1967; Luco *et al.*, 1987). More on the structural system is given by Kuroiwa (1967), Foutch *et al.* (1975), Foutch (1976), Luco *et al.* (1987), and Clinton (2004).

The building was first instrumented in 1968 with two permanent tri-axial accelerometers, located on the roof and the basement. A ten-channel strong-motion array was added to the instrumentation in 1979, with channels on the basement, the sixth floor, and the roof. After the 1994 Northridge, California, earthquake, the instrumentation was upgraded to a 36-channel, triggered system with three horizontals at each floor plus three verticals in the basement; the locations and directions of these are shown by the arrows in Figure 2. In 2000, the system was converted to a 19-bit real-time system recording continuously at 200 Hz. Also, a separate 24-bit tri-axial accelerometer was installed on the ninth floor recording continuously as a California Integrated Seismic Network (CISN, formerly TriNet) station MIK. (See www.cisn.org for

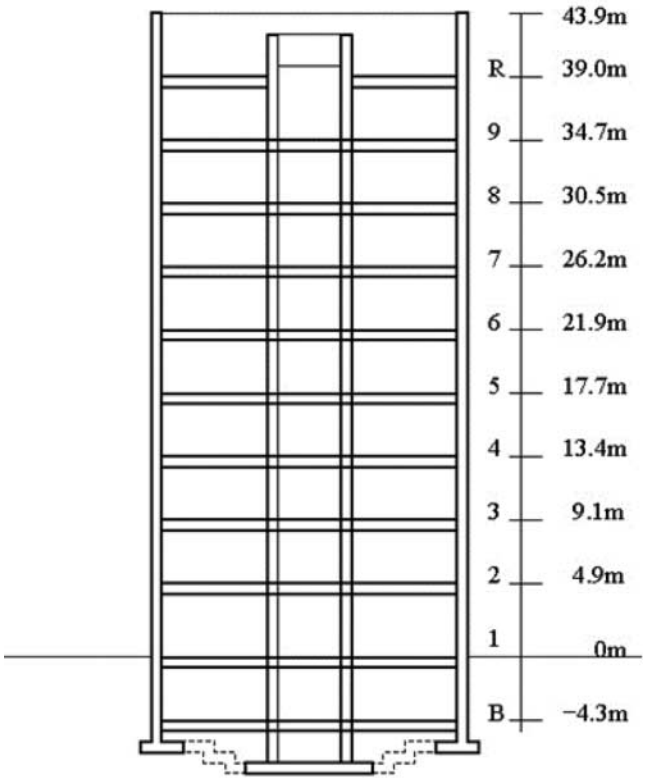

Figure 1. Vertical cross section of the Millikan Library in the north–south direction.

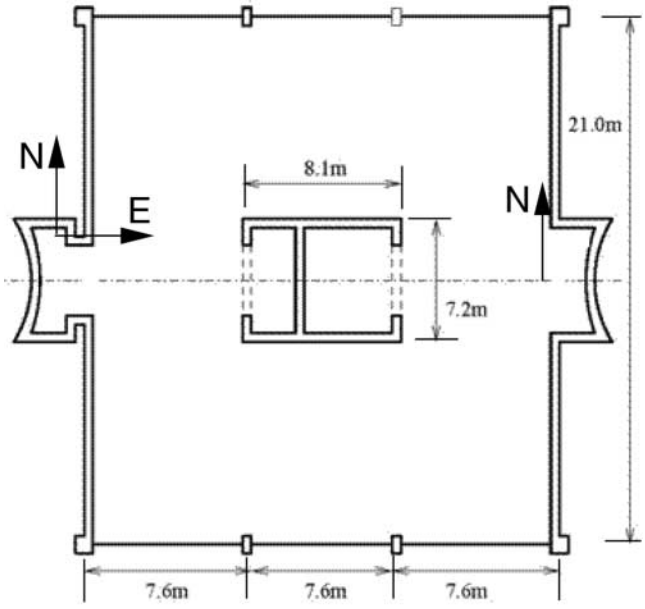

Figure 2. Floor plan of the Millikan Library. On floors 1–9 seismometers measure the motion in two horizontal directions on the west side of the building and the north–south motion on the east side, as indicated by the arrows.

more information on these networks.) Figure 2 shows the current sensor layout in the building.

Since its construction, the building has been a field laboratory for researchers in earthquake engineering. A synchronized shaker was permanently installed on the roof of the building in the early 1970s by M. D. Trifunac, which is still operational and used for forced vibration testing experiments (e.g., Foutch *et al.*, 1975; Wong *et al.*, 1977). Numerous studies on the dynamic behavior of the building have been completed by using vibration data from shaker experiments and real earthquakes (Kuroiwa, 1967; Trifunac, 1972; Udwadia and Trifunac, 1974; Luco *et al.*, 1986, 1987; Foutch *et al.*, 1975; Foutch, 1976; Foutch and Jennings, 1978; Clinton, 2004).

The acceleration in the north–south direction recorded at the west side of the building after the Yorba Linda earthquake of 3 September 2002 (M_L 4.8; time, 02:08:51 PDT; 33.917° N 117.776° W; depth, 3.9 km) is shown in Figure 3. The *P* waves generated by the earthquake arrive before $t = 9$ sec; these waves couple weakly to the horizontal motion in the building. The *S* wave that arrives at about $t = 11$ sec is the strongest phase. The surface waves that arrive later excite a resonance in the building with an amplitude that increases with the floor level.

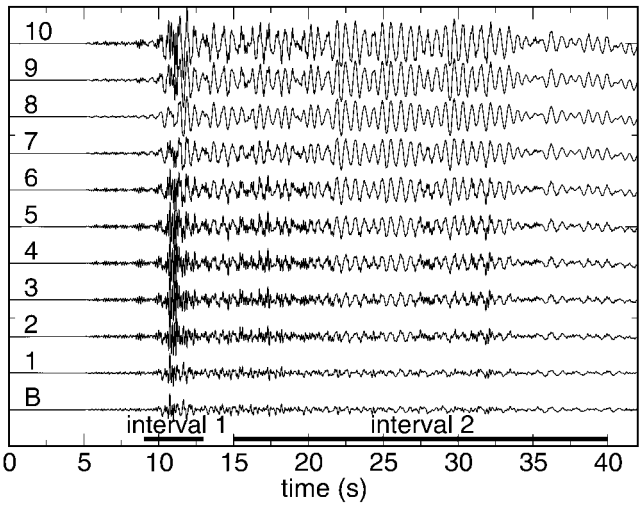

Figure 3. The north–south component of acceleration in the west side of the Millikan Library after the Yorba Linda earthquake of 3 September 2002 (M_L 4.8; time, 02:08:51 PDT; 33.917° N 117.776° W; depth, 3.9 km). The traces are labeled with the floor number (B indicates basement).

The Deconvolved Waveforms

In this study we extract the building response by deconvolving the waves recorded at all floors either with the waveform recorded in the basement or with the signal recorded at the top floor of the building. The deconvolution of two signals $u_1(\omega)$ and $u_2(\omega)$ is in the frequency domain given by

$$D(\omega) = u_1(\omega)/u_2(\omega). \quad (1)$$

This expression is unstable near the notches in the spectrum of u_2 because the denominator goes to zero. To stabilize the deconvolution we used the following estimator for the deconvolution instead:

$$D(\omega) = \frac{u_1(\omega)u_2^*(\omega)}{|u_2(\omega)|^2 + \varepsilon}, \quad (2)$$

where the asterisk denotes the complex conjugation. When $\varepsilon = 0$ this expression reduces to expression (1). In this study the parameter ε was set to 10% of the average spectral power.

The waveforms deconvolved with the signal recorded in the basement are shown in Figure 4. The deconvolved wave in the basement is a single spike because a signal deconvolved with itself is a delta function. The deconvolved waves at all the floors are causal, that is, they vanish for $t < 0$. The first onset of the deconvolved waves is a wave that propagates upward in the building. A reflection of this wave by the top of the building is visible as the second peak

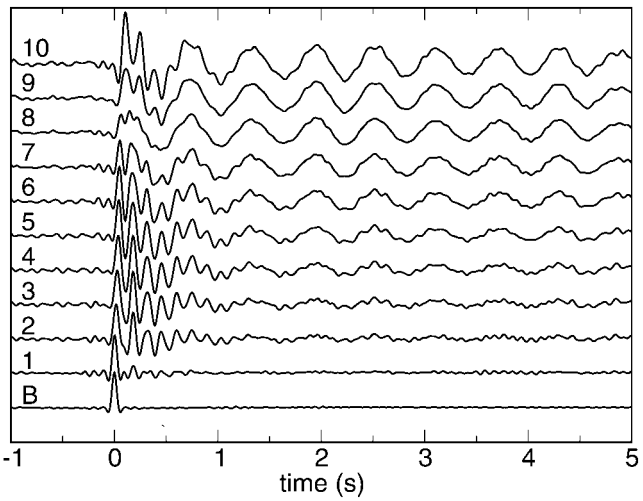

Figure 4. The waveforms of Figure 3 at the different floors after deconvolution with the waves recorded in the basement.

in the waves that propagates downward. The early part of the deconvolved waves consists of a superposition of upward- and downward-propagating waves. Because these waves interfere, it is difficult to identify the individual upward- and downward-propagating waves. The later part of the deconvolved waves consists of the resonance of the building. This resonance grows in amplitude with the floor level and is fairly monochromatic.

The waveforms deconvolved with the signal recorded in the basement are complicated. In contrast, as shown in Figure 5, the waveforms deconvolved with the signal recorded at the top floor are much simpler. These deconvolved

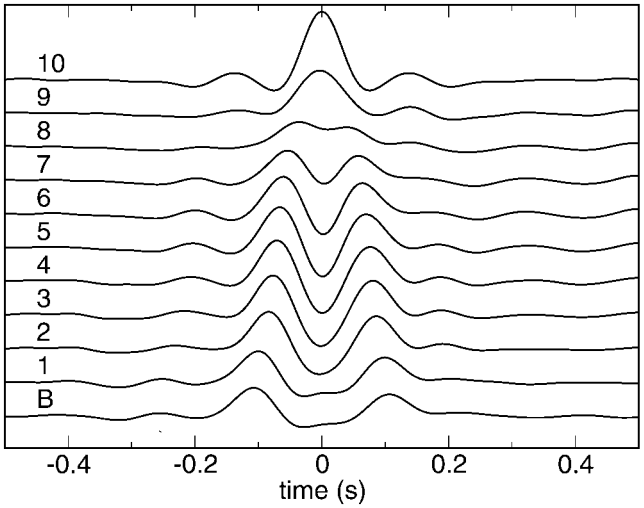

Figure 5. The waveforms of Figure 3 at the different floors after deconvolution with the waves recorded at the top floor.

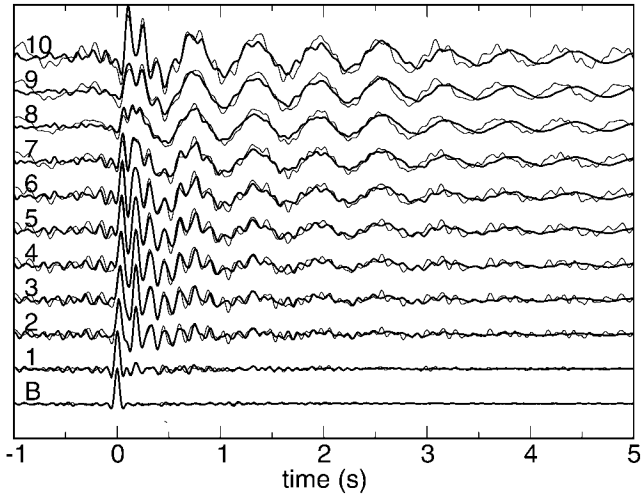

Figure 6. The waveforms of Figure 3 at the different floors after deconvolution with the waves recorded in the basement using only part of the data of Figure 3. The deconvolved waves shown in thick lines are obtained by using only the data in interval 1 of Figure 3, whereas the deconvolved waves shown in the thin lines are computed from the data in interval 2.

waves are acausal and consist of the superposition of one upgoing wave and one downgoing wave. The waves propagate, in general, in three directions through the building. The simplicity of the deconvolved waveforms suggests that the wave propagation is essentially one-dimensional for the employed frequencies. There is little indication that the upgoing and downgoing waves are reflected within the building. The reflection coefficients by the floors within the building (Şafak, 1999), therefore, must be small for the employed frequencies. The reflection coefficient for elastic waves by a floor in the building depends on the product of the frequency and the mass of the floor (Doyle, 1989; Şafak, 1999). This means that the absence of waves reflected off the floors in the building may be due to the relatively low frequencies in the waveforms used in this study. In addition, the dominant wavelength of the employed waves spans several floors; this further suppresses reflections generated by the individual floors because a medium with small-scale variations can be treated as an effective medium that behaves like a homogeneous medium with properties that are determined by the background velocity and the embedded scatterers (Tatarskiĭ and Gertsenshteiĭn, 1963; Keller and Karal, 1966; Frisch, 1968). For frequencies higher than employed here the floor spacing is larger than a wavelength; this may produce reflections by the individual floors.

The deconvolved waveforms in Figures 4 and 5 are computed from the full waveforms shown in Figure 3. It is, however, not necessary to use the full waveforms. We have also deconvolved the signals using the time intervals 1 and 2 shown in Figure 3. Interval 1 straddles the *S*-wave arrival and is 4 sec long, whereas interval 2 contains the surface-wave arrivals and has a duration of 25 sec. Both intervals were padded with zeroes to a duration of 40 sec. The signals deconvolved with the waves recorded in the basement for each of the intervals are shown in Figure 6. The thick line denotes the deconvolved waveforms from interval 1, whereas the thin line denotes the deconvolved waves from interval 2.

The similarity of the waves deconvolved over different intervals is striking. Note how the deconvolved waves from interval 1 display the resonance of the building, despite the fact that these waves are based on the impulsive *S*-wave arrival only. The broadband nature of the *S* wave ensures that sufficient low-frequency information is present to reproduce the resonance. Note also that the deconvolved waves from interval 2 are based on the surface-wave signal. Nevertheless, these deconvolved waves display the upward- and downward-propagating waves early in the deconvolved signal. The recorded waves in interval 2 are dominated by low-frequency surface waves. These waves visually mask the higher-frequency components in interval 2. The deconvolution equalizes the frequency content and therefore brings out the high-frequency propagating waves in Figure 6. Interval 1 is shorter than interval 2, and one might think that interval 1 therefore contains less information than interval 2. Because of the impulsive character of the *S* wave, the waves in interval 1 have a larger bandwidth than the waves in interval 2. This larger bandwidth helps stabilize the deconvolution. The similarity of the deconvolved waves for the intervals 1 and 2 shown in the Figures 6 and 7 suggests that for the level of shaking used in this study the building responds linearly. Moreover, the similarity of the deconvolved waveforms for intervals 1 and 2 indicate that the building response has not changed by the shaking by this event. This supports the assumption of a time-invariant response for this event. This assumption does not necessarily hold for ground motion with a higher intensity. Small differences in

deconvolved waves obtained from the two intervals can be due to the nonlinear response of the building.

The waves deconvolved with the signal recorded at the top floor for interval 1 and interval 2 is shown in Figure 7 with a thick and thin line, respectively. As in the preceding figure, these deconvolved waves are similar. This implies that the S wave and the surface wave both contain information about the upward- and downward-propagating waves in the building. The deconvolution defined in equation (2) and the choice of ε are not optimized. A more careful choice of the deconvolution algorithm could make the deconvolved waves from intervals 1 and 2 even more similar.

The deconvolved waves behave in the same way as a hologram. A part of a hologram can be used to reconstruct the image, albeit with a degraded resolution compared with the image of the full hologram (Lauterborn *et al.*, 1995). As shown in the Figures 6 and 7, the deconvolved waves that are computed from different subintervals of the whole signal lead to the same deconvolved waves.

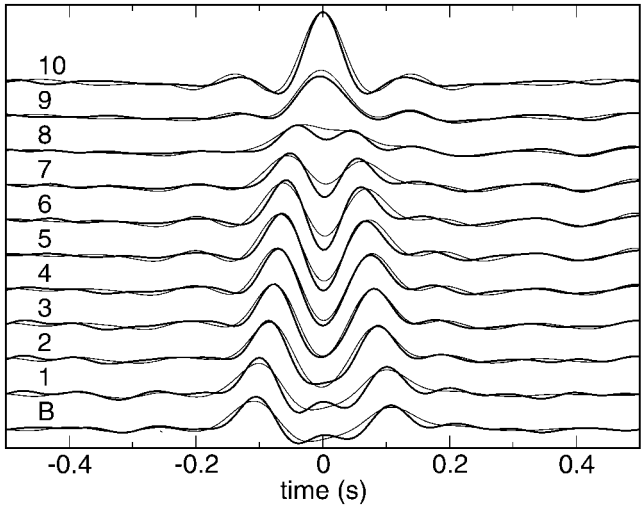

Figure 7. The waveforms of Figure 3 at the different floors after deconvolution with the waves recorded in the top floor using only part of the data of Figure 3. The deconvolved waves shown in thick lines are obtained by using only the data in interval 1 of Figure 3, whereas the deconvolved waves shown in the thin lines are computed from the data in interval 2.

Deconvolution Changes the Boundary Condition

We denote the motion at height z deconvolved with the motion at the top floor as $T(z, \omega)$, so that in the frequency domain

$$T(z, \omega) \equiv \frac{u(z, \omega)}{u(z = H, \omega)}. \tag{3}$$

Similarly, the motion deconvolved with the motion at the bottom floor as denoted by $B(z, \omega)$, hence,

$$B(z, \omega) \equiv \frac{u(z, \omega)}{u(z = 0, \omega)}. \tag{4}$$

We show in this section that the waveforms obtained by the deconvolution (4) satisfy a different boundary condition at the base of the building than the original waveforms do. The treatment in this section is applicable to tall buildings where the motion is essentially one-dimensional. It is not valid for broad buildings that are exposed to a lateral shear at the base (Trifunac, 1997).

As indicated in Figure 8 the waves near the base of the building can locally be decomposed in downgoing and upgoing waves

$$u(z, \omega) = A_-(\omega)e^{-ikz} + A_+(\omega)e^{ikz}. \tag{5}$$

The deconvolved wavefield defined in expression (4) can, locally, also be written as a superposition of upgoing and downgoing waves:

$$B(z, \omega) = C_-(\omega)e^{-ikz} + C_+(\omega)e^{ikz}, \tag{6}$$

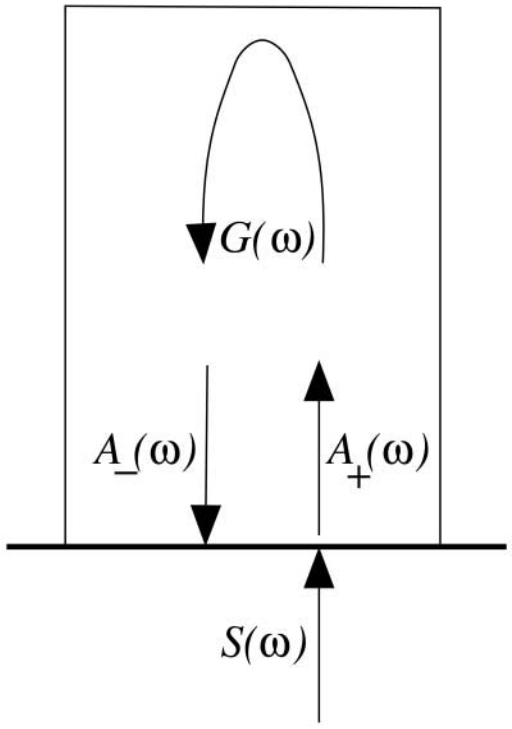

Figure 8. Sketch of the coefficients for upgoing and downgoing waves $A_\pm(\omega)$ at the base of the building, the building response $G(\omega)$ to an upgoing wave, and the excitation $S(\omega)$. The positive z direction is upward.

but the coefficients $C_{\pm}$ differ from $A_{\pm}$. Inserting the decomposition (5) into (4) gives

$$C_-(\omega) = \frac{A_-(\omega)}{A_-(\omega) + A_+(\omega)}, \qquad C_+(\omega) = \frac{A_+(\omega)}{A_-(\omega) + A_+(\omega)}. \tag{7}$$

In the following we denote the building response to an upgoing wave by $G(\omega)$, which accounts for the wave propagation within the building, including internal reflections and anelastic attenuation. The downgoing wave is related to the upgoing wave by

$$A_-(\omega) = G(\omega)A_+(\omega). \tag{8}$$

We assume the building is excited at the base by a shaking that is, in the frequency domain, denoted by $S(\omega)$, and the reflection coefficient at the base of the building is given by $R(\omega)$. The shaking $S(\omega)$ is the combined result of the ground motion in the free field, and the transfer of the ground motion to the base of the building. The coefficient for upward-going waves is equal to the sum of the excitation and upward-reflected wave at the base

$$A_+(\omega) = S(\omega) + R(\omega)A_-(\omega). \tag{9}$$

Solving expressions (8) and (9) for $A_{\pm}(\omega)$ gives

$$A_+(\omega) = \frac{S(\omega)}{1 - R(\omega)G(\omega)}, \qquad A_-(\omega) = \frac{G(\omega)S(\omega)}{1 - R(\omega)G(\omega)}. \tag{10}$$

A Taylor series of the denominator of $A_+(\omega)$ expresses the coefficient of the upgoing wave in the building as a sum of waves that are reflected repeatedly off the base of the building

$$A_+(\omega) = \{1 + R(\omega)G(\omega) + R^2(\omega)G^2(\omega) + \ldots\}S(\omega). \tag{11}$$

The term $R^n(\omega)$ corresponds to waves that are reflected n times off the base of the building. Inserting expression (10) for $A_{\pm}(\omega)$ into equation (7) for the coefficient $C_+(\omega)$ for the upgoing wave in the deconvolved wave field gives

$$C_+(\omega) = \frac{1}{1 + G(\omega)}. \tag{12}$$

This coefficient does not depend on the excitation $S(\omega)$; this is a natural result of the spectral division in expression (4). Note that $C_+(\omega)$ is also independent of the coefficient $R(\omega)$ for reflection off the base of the building. A Taylor series expansion of the denominator expresses $C_+(\omega)$ in the series

$$C_+(\omega) = 1 - G(\omega) + G^2(\omega) + \ldots. \tag{13}$$

This reverberation series is similar to the reverberation series (11) for the original wave field, but the reflection coefficient $R(\omega)$ in expression (11) is replaced by a reflection coefficient -1 in the series (13). Physically this means that the deconvolved wave field $B(z, \omega)$ corresponds to a wave state that is totally reflected off the base of the building.

It has been shown earlier that seismic interferometry can be used to determine waveforms for the system with different boundary conditions than the physical boundary conditions (Riley and Claerbout, 1976; Wapenaar *et al.*, 2004). Riley and Claerbout (1976) coined the phrase "Noah's deconvolution" for this principle.

The wave motion in the building is damped by intrinsic attenuation and by radiation damping at the base of the building. Radiation damping is accounted for by the condition $|R(\omega)| < 1$. As shown in the expansion (13) the deconvolved waves correspond to a wave state with reflection coefficient -1 at the base of the building. This means that the deconvolved wave field is not subject to radiation losses, and its decay with time depends on the intrinsic attenuation in the building only.

A Simple Model for the Wave Propagation in the Building

In this section we present a simple model for the wave propagation for the building. This model is similar to the shear-beam model proposed by Iwan (1977). The shear-beam model has been used to study various aspects of the building response to earthquakes (e.g., Anagnostopulos and Spiliopoulos, 1992; Hall *et al.*, 1995). The base of the building is exposed to an external motion $s(t)$ with Fourier transform $S(\omega)$. In this model, the wave propagates upward in the building with a velocity c that is the shear velocity of the building. At the top of the building with height H the waves are reflected with reflection coefficient $+1$. During the upward and downward propagation the waves attenuate; for a wave that travels over a distance L this is described by an attenuation operator $A(L, t)$. For a constant Q-model, this attenuation operator is in the frequency domain given by Aki and Richards (2002):

$$A(L, \omega) = \exp(-\gamma|\omega|L/c), \tag{14}$$

where the viscous damping ratio γ is related to the quality factor by

$$\gamma = 1/2Q. \tag{15}$$

The assumption of a viscous damping ratio, and quality factor, that is independent of frequency may not be realistic.

This assumption is, however, not essential in the following analysis because the viscous damping ratio can be an arbitrary function of frequency $\gamma(\omega)$ that satisfies causal energy dissipation. Kim and Collins (2002) describe different attenuation mechanisms for dynamic models similar to the one described here.

The downward-propagating waves reflect off the base of the building with a reflection coefficient $R(\omega)$ that corresponds in the time domain to a reflection operator $r(t)$. A wave $s(t)$ that travels upward in the building is given by $s(t - z/c)$. When the wave reflects off the top of the building, with reflection coefficient $+1$, the downgoing wave is given by $s(t - (2H - z)/c$. When this downgoing wave reflects off the base of the building, it is convolved with the reflection operator $r(t)$. The wave that then travels upward is given by $r(t) * s(t - (2H + z)/c)$. The delay time $2H/c$ accounts for the time needed to propagate once up and down the building. This process can be continued for all the upward- and downward-propagating waves and is similar to the treatment of water-layer reverberations of Backus (1959) and that of Love waves in a soft layer near the surface. After a convolution with the attenuation operators for each upward- and downward-going wave, the total response of the building is in the time domain given by

$$u(z,\,t) \;=\; A(z,\,t) * s\left(t \,-\, \frac{z}{c}\right) \,+\, A(2H \,-\, z,\,t) * s\left(t \,-\, \frac{2H \,-\, z}{c}\right) \\ +\; r(t) * A(2H \,+\, z,\,t) * s\left(t \,-\, \frac{2H \,+\, z}{c}\right) \,+\, r(t) * A(4H \,-\, z,\,t) * s\left(t \,-\, \frac{4H \,-\, z}{c}\right) \,+\, \ldots \tag{16}$$

This sum of upgoing and downgoing waves is similar to the uniform shear beam model used by Iwan (1997). With the wavenumber defined by

$$k \;=\; \omega/c\,, \tag{17}$$

and for the attenuation model (14), this expression is in the frequency domain given by

$$u(z,\,\omega) \;=\; \sum_{n=0}^{\infty} S(\omega)R^n(\omega)\,\left\{e^{ik(2nH+z)}e^{-\gamma|k|(2nH+z)} \right. \\ \left. +\; e^{ik(2(n+1)H-z)}e^{-\gamma|k|(2(n+1)H-z)}\right\}. \tag{18}$$

In this expression n counts the number of bounces off the base of the building. The first term denotes the upward-propagating waves, whereas the last term accounts for the downward-propagating waves that have bounced n times in the building.

Let us first analyze the deconvolution with respect to the motion at the highest floor. Inserting expression (18) in the numerator and denominator of the definition (3) gives

$$T(z,\,\omega) \;=\; \frac{\sum_{n=0}^{\infty} S(\omega)R^n(\omega)\,\left\{e^{ik(2nH+z)}e^{-\gamma|k|(2nH+z)} \,+\, e^{ik(2(n+1)H-z)}e^{-\gamma|k|(2(n+1)H-z)}\right\}}{2\sum_{n=0}^{\infty} S(\omega)R^n(\omega)\; e^{ik(2n+1)H}e^{-\gamma|k|(2n+1)H}}. \tag{19}$$

This expression can also be written as:

$$T(z,\,\omega) \;=\; \frac{\left\{e^{ik(z-H)}e^{-\gamma|k|(z-H)} \,+\, e^{ik(H-z)}e^{-\gamma|k|(H-z)}\right\}\,\sum_{n=0}^{\infty} S(\omega)R^n(\omega)e^{ik(2n+1)H}e^{-\gamma|k|(2n+1)H}}{2\sum_{n=0}^{\infty} S(\omega)R^n(\omega)\; e^{ik(2n+1)H}e^{-\gamma|k|(2n+1)H}}. \tag{20}$$

The excitation $S(\omega)$ and the sum with the reverberations in the numerator and the denominator cancel, so that

$$T(z,\omega) \;=\; \frac{1}{2}\,\left\{e^{ik(z-H)}e^{-\gamma|k|(z-H)} \,+\, e^{ik(H-z)}e^{-\gamma|k|(H-z)}\right\}. \tag{21}$$

This means that $T(z,\,\omega)$ accounts for the sum of one attenuating upgoing wave and one downgoing wave. Because $z < H$, the upgoing wave is acausal. The cancellation of the sum over reverberations means that $T(z,\,\omega)$ is independent of the reverberations in the building. The cancellation of the reflection coefficient $R(\omega)$ implies that $T(z,\,\omega)$ does not depend on the coupling of the building to the subsurface. The cancellation of $S(\omega)$ means that the deconvolved response in independent of the excitation of the building.

A similar analysis can be applied to the building response deconvolved with the motion at the base. Inserting expression (18) in the numerator and denominator of expression (4) gives

$$B(z,\ \omega)\ =\ \frac{\sum_{n=0}^{\infty}\ S(\omega)R^n(\omega)\ \left\{e^{ik(2nH+z)}e^{-\gamma|k|(2nH+z)}\ +\ e^{ik(2(n+1)H-z)}e^{-\gamma|k|(2(n+1)H-z)}\right\}}{\sum_{n=0}^{\infty}\ S(\omega)R^n(\omega)\ \left\{e^{ik2nH}e^{-\gamma|k|2nH}\ +\ e^{ik2(n+1)H}e^{-\gamma|k|2(n+1)H}\right\}}. \qquad (22)$$

Factoring out the summations this can be written as

$$B(z,\ \omega)\ =\ \frac{\left\{e^{ikz}e^{-\gamma|k|z}\ +\ e^{ik(2H-z)}e^{-\gamma|k|(2H-z)}\right\}\ \sum_{n=0}^{\infty}\ S(\omega)R^n(\omega)e^{ik2nH}e^{-\gamma|k|2nH}}{\left\{1\ +\ e^{2ikH}e^{-2\gamma|k|H}\right\}\ \sum_{n=0}^{\infty}\ S(\omega)R^n(\omega)\ e^{ik2nH}e^{-\gamma|k|2nH}}. \qquad (23)$$

The summation over the reverberations, the reflection coefficient $R(\omega)$, and the excitation $S(\omega)$ cancel, so that

$$B(z,\ \omega)\ =\ \frac{e^{ikz}e^{-\gamma|k|z}\ +\ e^{ik(2H-z)}e^{-\gamma|k|(2H-z)}}{1\ +\ e^{2ikH}e^{-2\gamma|k|H}}. \qquad (24)$$

Just as for the signals deconvolved with the top floor, this deconvolved signal depends neither on the coupling with the ground nor on the excitation.

The deconvolved response $T(z,\ \omega)$ is the superposition of one acausal upgoing wave and one causal downgoing wave. Such a simple interpretation cannot be applied to $B(z,\ \omega)$ because the numerator depends on frequency. The deconvolved response can be interpreted in two ways: as a superposition of traveling waves, or as a superposition of modes. The traveling-wave interpretation is obtained by using the following geometric series:

$$\frac{1}{1\ +\ e^{2ikH}e^{-2\gamma|k|H}}\ =\ \sum_{n=0}^{\infty}\ (-1)^n\ e^{2iknH}e^{-2\gamma|k|nH}. \qquad (25)$$

Because of the attenuation, this sum is guaranteed to converge. Inserting this in equation (24) gives $B(z,\ \omega)$ as an infinite sum of upgoing and downgoing traveling waves:

$$B(z,\ \omega)\ =\ \sum_{n=0}^{\infty}\ (-1)^n\ \left\{e^{ik(z+2nH)}e^{-\gamma|k|(z+2nH)}\right.$$
$$\left.+\ e^{ik(2(n+1)H-z)}e^{-\gamma|k|(2(n+1)H-z}\right\}. \qquad (26)$$

The difference from expression (24) is that the frequency-dependent denominator has disappeared. Note that because the argument of each of the complex exponentials is positive, $B(z,\ \omega)$ is a causal function. This deconvolved response is an infinite sum of upgoing and downgoing attenuated waves. This sum differs from the sum of upgoing and downgoing waves in the building, because $B(z,\ \omega)$ does not depend on the ground coupling, whereas the original sum of upgoing and downgoing waves (18) does depend on the ground coupling through the reflection coefficient $R(\omega)$.

In expression (26) the number of bounces off the base is given by the summation index n. Each bounce gives a contribution $(-1)^n$. As shown in the section Deconvolution Changes the Boundary Condition for a general building response, a reflection of the deconvolved waves off the base of the building corresponds to a reflection coefficient -1 rather than the reflection coefficient $R(\omega)$ caused by the subsurface at the base of the physical building. There is a simple explanation for this (J. Sheiman, personal comm., 2004). The deconvolution of the motion of the basement with itself gives, by definition, a bandpass-filtered delta function as shown in the bottom trace of Figure 4. When the wave that has reflected off the top of the building propagates downward, it gives a vanishing contribution at the base of the building because the deconvolved wave at that level vanishes for $t > 0$. The motion at the base can only vanish when an upward-propagating wave is launched with the opposite polarity to the downward propagating wave that strikes the basement. This corresponds to a reflection coefficient for the deconvolved waves that is equal to -1 rather than the reflection coefficient $R(\omega)$ of the subsurface.

An alternative way to interpret $B(z,\ \omega)$ is based on normal modes (Chopra and Chintanapadkee, 2001). Using the inverse Fourier transform and expression (17), the deconvolved response is in the time domain given by

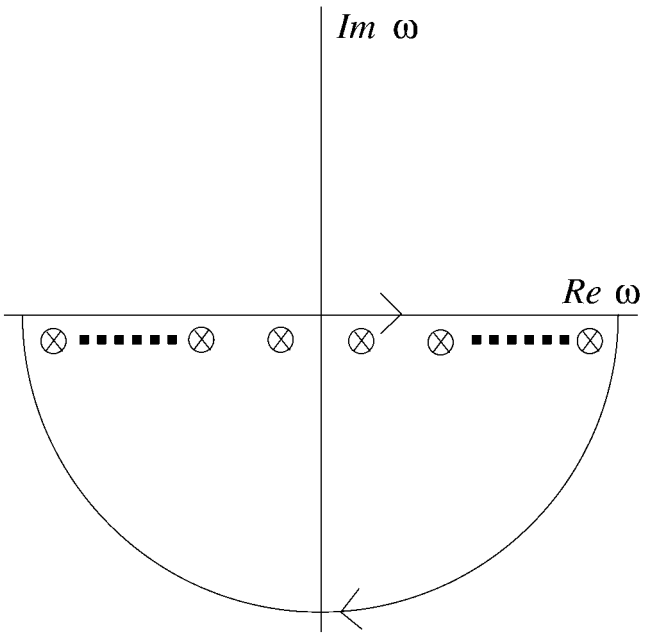

Figure 9. The location of the poles in the complex ω plane and the contour integration that is used for $t > (2H - z)/c$.

$$B(z,\,t)\;=\;\int_{-\infty}^{\infty}\frac{e^{-i\omega(t-z/c)}e^{-\gamma|\omega|z/c}\;+\;e^{-i\omega(t-(2H-z)/c)}e^{-\gamma|\omega|(2H-z)/c}}{1\;+\;e^{2i\omega H/c}e^{-2\gamma|\omega|H}}\,d\omega. \qquad (27)$$

We show in the appendix that this integral can be solved by contour integration. The integrand has simple poles when

$$1\;+\;e^{2i\omega H/c}e^{-2\gamma|\omega|H}\;=\;0, \qquad (28)$$

the location of the poles in the lower half-plane is shown in Figure 9. For $t > (2H - z)/c$, the contour must be closed in the lower half-plane, and as shown in the appendix the integral (27) can be written as a sum of damped normal modes:

$$B(z,\,t)\;=\;\frac{4\pi c}{H}\sum_{m=0}^{\infty}(-1)^{m+1}\exp(-\gamma\omega_m t)\,\cos\!\left(\frac{\omega_m(H\;-\;z)}{c}\right)\sin(\omega_m t), \qquad (29)$$

with

$$\omega_m\;=\;\frac{(m\;+\;1/2)\pi c}{H},\quad m\;=\;0,\,1,\,2,\,\ldots \qquad (30)$$

Note that these normal modes are not the normal modes of the building, because its normal modes also depend, in general, on the coupling to the ground (Trifunac *et al.*, 2001a,b, 2003). The normal modes in the sum (29) are independent of the reflection coefficient $R(\omega)$; hence, the normal modes in the deconvolved response depend on the properties of the building only. This is consistent with the traveling-wave formulation of expression (26), where the reflection coefficient for the deconvolved wave is equal to -1 rather than the reflection coefficient $R(\omega)$ of the subsurface. The normal mode frequencies (30) correspond to those of a shear beam that is clamped at one end.

Each term in the sum (29) is exponentially damping. The term with the fundamental mode ($m = 0$) has the smallest damping. This means that for large times ($t \gg 2H/\pi c$) the fundamental mode dominates; hence,

$$B(z,\,t)\;\approx\;\frac{4\pi c}{H}\exp(-\gamma\omega_0 t)\,\cos\!\left(\frac{\omega_0(H\;-\;z)}{c}\right)\sin(\omega_0 t), \qquad (31)$$

with

$$\omega_0\;=\;\frac{\pi c}{2H}. \qquad (32)$$

The period that corresponds to this angular frequency is given by

$$T_0\;=\;\frac{4H}{c}. \qquad (33)$$

Note that this is the time needed to propagate up and down the building twice. This period is determined by the factor $(-1)^m$ in expression (26). Because of this factor the wave changes polarity if it propagates up and down the building once. If the wave travels up and down the building twice and covers a distance $4H$, the polarity changes twice and the reverberating wave reinforces itself to form a resonance.

Interpretation of the Deconvolved Waveforms

The theory of the preceding section agrees with the deconvolved waves in the Figures 4 and 5. Let us first consider the waves deconvolved with the waves at the top floor as shown in Figure 5. These deconvolved waves are given by expression (21) that gives the superposition of an acausal upgoing wave and a causal downgoing wave; both waves are clearly visible in Figure 5. Given the floor spacing of 4.27 m (Clinton, 2004) these waves can be used to estimate the shear velocity in the building. It follows from expression (21) that if there is no attenuation ($\gamma = 0$), and if the data have infinite bandwidth, that the deconvolution is in the time domain given by a superposition of upward- and downward-propagating delta functions:

$$T(z,\,t)\;=\;\pi\left\{\delta\!\left(t\;-\;\frac{z\;-\;H}{c}\right)\;+\;\delta\!\left(t\;+\;\frac{z\;-\;H}{c}\right)\right\}. \qquad (34)$$

(Expression 17 is used in deriving this result.) The attenuation and the finite bandwidth of the data cause the broader pulses shown in Figure 5.

We measured the arrival time of the upward- and downward-propagating waves by picking the maximum of these waves. These arrival times are shown in Figure 10. The distance is measured relative to the position of the accelerometer at the top floor. For the upward-propagating wave this distance is given a negative value. For floors 4–10 the upward- and downward-propagating waves overlap. This may bias the travel-time measurements. The travel times at these floors are indicated with open squares. The travel time determined from the waves recorded in the basement may be biased by the presence of the solid earth below the basement; these travel times are also indicated with open squares. Despite these reservations, the measurements in Figure 10 display a fairly linear dependence of the travel time with distance; this indicates a constant shear velocity in the building.

According to expression (21), the upward- and downward-propagating waves both decay due to attenuation. This attenuation can be seen in Figure 5 because the downward-going wave has a consistently smaller amplitude than the upward-propagating wave. The absolute value of the amplitude at different floors cannot be compared with great ac-

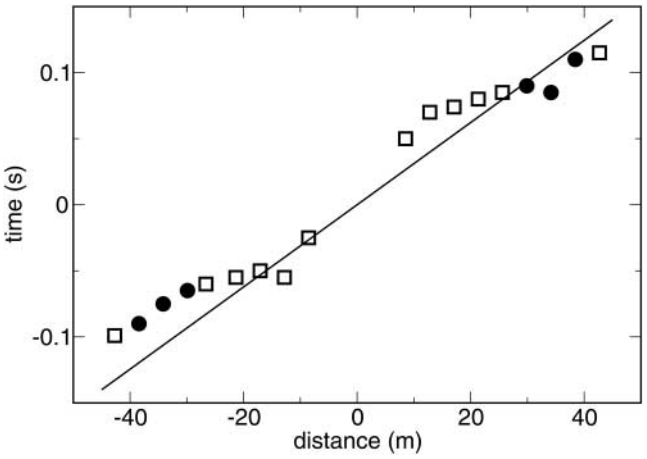

Figure 10. The arrival times of the upgoing and downgoing waves in Figure 5. A negative distance/time corresponds to the upgoing wave, a positive distance/time to the downgoing wave. The travel times at floors 1–3 are marked with solid circles. The solid line indicates the travel time predicted for the shear velocity inferred from the normal-mode measurements that give a velocity of 322 m/sec.

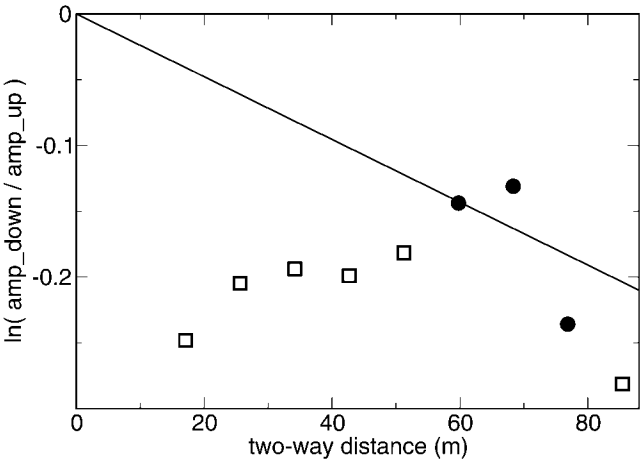

Figure 11. The natural logarithm of the ratio of the amplitudes of the upgoing and downgoing waves of Figure 5 as a function of the two-way distance to the top of the building. The amplitude ratio for floors 1–3 is indicated with solid circles. The log-amplitude ratio predicted by the attenuation of expression (37) is shown with the straight line.

curacy, because the absolute amplitude is affected by the receiver coupling and other uncertainties. The ratio of the amplitude of the downgoing wave and the upgoing wave, however, does not depend on the receiver coupling. Figure 11 shows the natural logarithm of the ratio of the downgoing wave and the upgoing wave at each floor. The amplitude measurements in floors 4–10 and in the basement are likely to be unreliable because of the interference of the upgoing and downgoing waves and the presence of the solid earth below the basement, respectively. The amplitude ratios at these levels are indicated with open squares. The amplitude ratio for floors 1–3 is indicated by solid circles and are most reliable. The two-way distance is measured relative to the receiver at the top floor. The scatter in the amplitude ratio is considerable because the amplitude difference between the upgoing and downgoing waves is fairly small. In a taller building these amplitude differences would be larger, and the attenuation can be determined with greater accuracy.

According to expressions (26) and (29), the signals deconvolved with the bottom floor can be seen either as a superposition of upward- and downward-propagating waves, or as a sum of normal modes. The interpretation in terms of propagating waves is most useful for the early part of the deconvolved waves in Figure 4. In that figure, the upward- and downward-propagating waves are not as clear as in Figure 5 for the waves deconvolved with the signals at the top floor, because in Figure 4 only one upgoing wave and one downgoing wave are present, whereas according to expression (26) many upgoing and downgoing waves interfere with each other in Figure 4. For this reason we analyze the waves deconvolved with the signal in the basement in Figure 4 from the normal mode point of view as formulated in expression (29). Because the fundamental mode is much stronger than the higher modes, we use the expressions (31), (32), (33) in the following.

The amplitude spectrum of the deconvolved waves of Figure 4 averaged over all the floors has a pronounced peak at 1.72 Hz. This reflects the monochromatic nature of the resonance. Given that the height of the building measured to the basement is 47 m, this gives with expression (33) a shear velocity of

$$c = 322 \text{ m/sec.} \tag{35}$$

The travel time as a function of distance for this velocity is indicated by the solid line in Figure 10. The proximity of this travel time curve to the arrival times of the upward- and downward-propagating waves, shows that the traveling waves and the normal modes predict a shear velocity that is similar. This provides a consistency check on the analysis. A systematic difference between the velocity of the propagating waves and the normal modes can be due to dispersion caused by the internal structure in the building (e.g., Todorovska *et al.*, 1988, 2001a, b), and to amplitude variations between floors that are ignored in expression (15) that forms the basis of the mathematical model in section A Simple Model for the Wave Propagation in the Building.

According to expression (31) the resonance decays with time because of anelastic attenuation. To quantify the attenuation we bandpass filtered the deconvolved waves of Figure 4 with a Butterworth filter with cutoff frequencies of 1 and 3 Hz, respectively. This filter extracts the fundamental mode from the waveforms. The natural logarithm of the envelope of the bandpass-filtered waveforms is shown in Figure 12. Since the modal amplitude is weak for the lowest

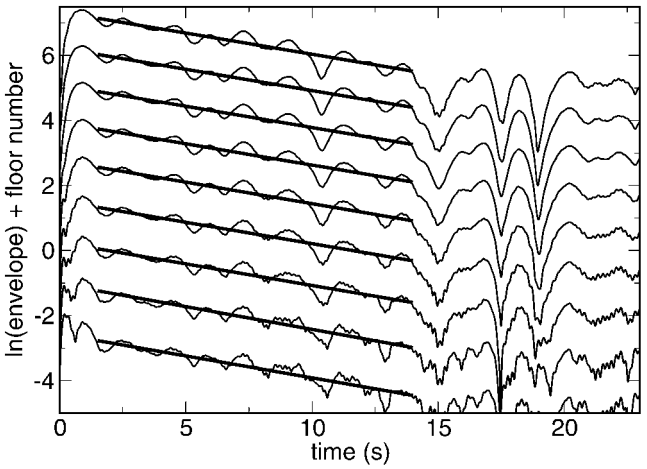

Figure 12. The natural logarithm of the envelope of the deconvolved waves in Figure 4 after applying a bandpass filter with corner frequencies of 1 Hz and 3 Hz, respectively. For clarity the floor number is added to each curve. The best-fitting straight line to each curve is indicated with thick solid lines.

floor, we used only the top nine floors in the normal-mode analysis. We added the floor number to each curve to separate them in the figure. Because only the slope depends on the attenuation, this offset does not affect the analysis. Note that, apart from some fluctuations, the envelope of the deconvolved waves decays with time. This contrasts the original waveforms in Figure 4 that do not decay with time because the motion is continuously excited by the surface waves. The deconvolution extracts the decay of the resonance with time, this makes it possible to measure the anelastic attenuation in the building.

Between 1.5 and 14 sec the logarithm of the envelope decays linearly with time, this is consistent with the exponential decay in expression (31). For later times the resonance is of the same order of magnitude as the ambient noise, and the exponential decay is not valid. To determine the attenuation we fitted straight lines to the curves for 1.5 sec $< t <$ 14 sec. The least-squares fit of the envelopes is shown by the solid lines in Figure 12. The slopes are similar and the average slope is given by

$$\text{Slope} = -0.1321 \pm 0.0017 \text{ sec}^{-1}. \qquad (36)$$

The error is determined by the standard deviation of the slope for the deconvolved waves at different floors. According to the expressions (15) and (31) the slope is equal to $-\omega/2Q$. For the resonant frequency of 1.72 Hz, this gives

$$Q = 20.45. \qquad (37)$$

This value of the attenuation can be compared with the attenuation of the propagating waves shown in Figure 11. The propagating waves in Figure 5 have a dominant frequency of about $f = 5$ Hz. The propagating waves decay with distance as $\exp(-\pi fz/Qc)$. For the value of Q given previously, and a velocity of 322 m/sec, this decay is shown by the solid line in Figure 11. The variability in the amplitude measurements in that figure is fairly large. For the lower three floors, where the upgoing and downgoing waves do not overlap and their amplitude ratio can be measured reliably, the attenuation inferred from the resonance agrees well with amplitude decay determined from the propagating waves as indicated with the solid circles. The comparison of the attenuation from the normal modes and the propagating waves provides a consistency check on the model of wave propagation employed in the building.

Discussion

We have shown that the deconvolution of the motion recorded at different floors in the building is an effective tool for extracting the building response and for separating intrinsic attenuation from radiation damping. The deconvolution with respect to the signals recorded in the basement and the top floor provides complementary information. The deconvolution with the signal recorded at the top floor gives one upgoing and one downgoing propagating wave that clearly are separated. The deconvolution with the waveforms recorded in the basement provides information on the fundamental mode of the building.

The deconvolved waves are independent of the excitation and of the ground coupling. This can be seen in expressions (21) and (24) that are independent of the excitation $S(\omega)$ and the reflection coefficient $R(\omega)$ at the base of the building. Suppose that instead of the deconvolution we had used the correlation, as is common in seismic interferometry (Lobkis and Weaver, 2001; Derode *et al.*, 2003; Snieder, 2004a; Wapenaar, 2004; Wapenaar *et al.*, 2005; Snieder *et al.*, 2006). In the frequency domain, the correlation of the waves recorded at height z with those in the basement is given by

$$C(z, \omega) = u(z, \omega)u^*(z = 0, \omega). \qquad (38)$$

When equation (18) is inserted in this expression, the result contains the power spectrum $|S(\omega)|^2$ of the excitation and products of the reflection coefficient $R(\omega)$. In contrast to this, the deconvolved waves of expressions (21) and (24) depend on neither of these quantities.

Expression (21) can be generalized for *SH* waves in an arbitrary-layered medium. In this case the deconvolved waves $T(z, \omega)$ are equal to the P_{11}-element of the propagator matrix (Trampert *et al.*, 1993). This contrasts formulations of seismic interferometry based on correlation where the Green's function is obtained (Lobkis and Weaver, 2001; Derode *et al.*, 2003; Snieder, 2004a; Wapenaar, 2004; Wapenaar *et al.*, 2005; Snieder *et al.*, 2006). According to expression (7.43) of Aki and Richards (2002), the P_{11}-element of the propagator matrix for *SH* waves in a lossless homogeneous medium is given by

$$P_{11}(z, H) = \cos k(z - H) = \frac{1}{2}\left(e^{ik(z-H)} + e^{ik(H-z)}\right). \quad (39)$$

Apart from terms that depend on the attenuation, this expression is identical to equation (21). We can show that this is also the case for a general layered medium that has internal reflections.

The deconvolved waves can be used to estimate the shear velocity and attenuation in the Millikan Library. The waves deconvolved with the motion in the top floor lead to clear upgoing and downgoing waves. The velocity of propagation can be measured from the arrival time of these waves, whereas the ratio of the amplitude of the upgoing and downgoing waves constrains the attenuation. The waveforms obtained by deconvolution with the motion in the basement gives the motion of the fundamental mode of the building. The frequency and temporal decay constrain the shear velocity and attenuation as well. As shown in Figures 10 and 11, these complementary pieces of information are consistent. This shows that the deconvolution of the motion in the building recorded at different levels can be used successfully to eliminate the imprint of the excitation and the ground coupling and that the values of the shear velocity and attenuation from propagating waves and the fundamental mode are consistent.

The motion shown in Figure 3 depends on the strength of the shaking. The deconvolved waves are independent of the excitation, if the building response is linear. The linearity of the building response can therefore be investigated by comparing the deconvolved waveforms for events with different strengths.

Acknowledgments

We appreciate the insights that we obtained from discussions with Jon Sheiman, Rodney Calvert, Huub Douma, Ken Larner, and Matt Haney, and we thank M.D. Trifunac and an anonymous reviewer for the critical and constructive comments.

References

Anagnostopulos, S. A., and K. V. Spiliopoulos (1992). An investigation of earthquake induced pounding between adjacent buildings. *Earthquake Eng. Struct. Dun.* **21,** 289–302.

Aki, K., and P. G. Richards (2002). *Quantitative Seismology*, Second Ed., Univ. Science Books, Sausalito, California.

Backus, M. M. (1959). Water reverberations—their nature and elimination, *Geophysics* **24,** 233–261.

Chopra, A. K., and C. Chintanapadkee (2001). Drift spectrum vs. modal analysis of structural response to near-fault motions, *Earthquake Spectra* **17,** 221–234.

Clinton, J. F. (2004). Modern digital seismology—instrumentation, and small amplitude studies in the engineering world, *Ph.D. Thesis*, California Institute of Technology.

Derode, A., E. Larose, M. Campillo, and M. Fink (2003). How to estimate the Green's function for a heterogeneous medium between two passive sensors? Application to acoustic waves, *Appl. Phys. Lett.* **83,** 3054–3056.

Doyle, J. F. (1989). *Wave Propagation in Structures: An FFT-Based Spectral Analysis Methodology*, Springer, New York.

Foutch, D. A. (1976). A study of the vibrational characteristics of two multistorey buildings, *Ph.D. Thesis*, California Institute of Technology.

Foutch, D. A., and P. C. Jennings (1978). Foundation response of a nine-storey reinforced concrete building, *Bull. Seism. Soc. Am.* **68,** 219–229.

Foutch, D. A., J. E. Luco, M. D. Trifunac, and M. E. Udwadia (1975). Full scale, three dimensional tests of structural deformation during forced excitation of a nine-storey reinforced concrete building, in *Proc. U.S. National Conference on Earthquake Engineering*, Ann Arbor, 206–215.

Frisch, U. (1968). Wave propagation in random media, in *Probabilistic Methods in Applied Mathematics*, A. T. Bharucha-Reid (Editor), Academic Press, New York, 75–198.

Hall, J. F., T. H. Heaton, M. W. Halling, and D. J. Wald (1995). Near-source ground motion and its effect on flexible buildings, *Earthquake Spectra* **11,** 569–605.

Iwan, W. D. (1997). Drift spectrum: measure if demand for earthquake ground motions, *J. Struct. Eng.* **123,** 367–404.

Keller, J. B., and F. C. Karal (1966). Effective dielectric constant, permeability, and conductivity of a random medium and the velocity and attenuation coefficient of coherent waves, *J. Math. Phys.* **7,** 661–670.

Kim, K., and K. R. Collins (2002). Closer look at the drift demand spectrum, *J. Struct. Eng.* **128,** 942–945.

Kuroiwa, J. H. (1967). Vibration test of a multistorey building, *Ph.D. Thesis*, California Institute of Technology.

Lauterborn, W., T. Kurz, and M. Wiesenfeldt (1995). *Coherent Optics, Fundamentals and Applications*, Springer-Verlag, Berlin.

Lobkis, O. I., and R. L. Weaver (2001). On the emergence of the Green's function in the correlations of a diffuse field, *J. Acoust. Soc. Am.* **110,** 3011–3017.

Luco, J., M. Trifunac, and H. Wong (1987). On the apparent change in dynamic behavior of a 9-story reinforced-concrete building, *Bull. Seism. Soc. Am.* **77,** 1961–1963.

Luco, J. E., H. L. Wong, and M. D. Trifunac (1986). Soil-structure interaction effects on forced vibration tests, Technical Report 86-05, University of Southern California, Department of Civil Engineering, Los Angeles, California.

Riley, D. C., and J. F. Claerbout (1976). 2-D multiple reflections, *Geophysics* **41,** 592–620.

Şafak, E. (1995). Detection and identification of soil-structure interaction in buildings from vibration recordings, *J. Struct. Eng.* **121,** 899–906.

Şafak, E. (1999). Wave-propagation formulation of seismic response of multistory buildings, *J. Struct. Eng.* **125,** 426–437.

Snieder, R. (2004a). Extracting the Green's function from the correlation of coda waves: a derivation based on stationary phase, *Phys. Rev. E* **69,** 046610.

Snieder, R. (2004b). *A Guided Tour of Mathematical Methods for the Physical Sciences*, Second Ed., Cambridge Univ. Press, Cambridge, United Kingdom.

Snieder, R., K. Wapenaar, and K. Larner (2006). Spurious multiples in interferometric imaging of primaries, *Geophysics* (in press).

Tatarskiĭ, V. I., and M. E. Gertsenshteiĭ (1963). Propagation of waves in a medium with strong fluctuations in refractive index, *Soviet Phys. JETP* **17,** 458–463.

Todorovska, M. I., S. S. Ivanović, and M. D. Trifunac (2001a). Wave propagation in a seven-story reinforced concrete building. I. Theoretical models, *Soil Dyn. Earthquake Eng.* **21,** 211–223.

Todorovska, M. I., S. S. Ivanović, and M. D. Trifunac (2001b). Wave propagation in a seven-story reinforced concrete building. II. Observed wavenumbers, *Soil Dyn. Earthquake Eng.* **21,** 225–236.

Todorovska, M. I., V. W. Lee, and M. D. Trifunac (1988). Investigation of earthquake response of long buildings, *USC Report* CE 88-02.

Trampert, J., M. Cara, and M. Frogneux (1993). *SH* propagator matrix and Q_s estimates from borehole- and surface-recorded earthquake data, *Geophys. J. Int.* **112,** 290–299.

Trifunac, M. D. (1972). Comparisons between ambient and forced vibration experiments, *Int. J. Earthquake Eng. Struct. Dyn.* **1,** 133–150.

Trifunac, M. D. (1997). Relative earthquake motion of building foundations, *J. Struct. Eng.* **123,** 414–422.

Trifunac, M. D., S. S. Ivanović, and M. I. Todorovska (2001a). Apparent periods of a building. I: Fourier analysis, *J. Struct. Eng.* **127,** 517–526.

Trifunac, M. D., S. S. Ivanović, and M. I. Todorovska (2001b). Apparent periods of a building. II: Time-frequency analysis, *J. Struct. Eng.* **127,** 527–537.

Trifunac, M. D., S. S. Ivanović, and M. I. Todorovska (2003). Wave propagation in a seven-story reinforced concrete building. III. Damage detection via changes in wavenumbers, *Soil Dyn. Earthquake Eng.* **23,** 65–75.

Udwadia, F. E., and M. D. Trifunac (1974). Time and amplitude dependent response of structures, *Int. J. Earthquake Eng. Struct. Dyn.* **2,** 359–378.

Wapenaar, K. (2004). Retrieving the elastodynamic Green's function of an arbitrary inhomogeneous medium by cross correlation, *Phys. Rev. Lett.* **93,** 254301.

Wapenaar, K., J. Fokkema, and R. Snieder (2005). Retrieving the Green's function by cross-correlation: a comparison of approaches, *J. Acoust. Soc. Am.* **118,** 2783–2786.

Wapenaar, K., J. Thorbecke, and D. Dragonov (2004). Relations between reflection and transmission responses of three-dimensional inhomogeneous media, *Geophys. J. Int.* **156,** 179–194.

Wong, H. L., M. D. Trifunac, and B. Westermo (1977). Effects of surface and subsurface irregularities on the amplitude of monochromatic waves, *Bull. Seism. Soc. Am.* **67,** 353–368.

Appendix

Evaluation of the Fourier Integral (27)

In this appendix we evaluate the Fourier integral (27) by using complex integration. For $t > (2H - z)/c$ the integration along the real ω axis must be closed in the lower half-plane to obtain a vanishing contribution of the semicircular integration path that is added in the contour integration (Snieder, 2004b). The value of the contour integral over the path shown in Figure 9 is determined by the poles of the integrand in expression (27) in the lower half-plane. The pole positions are determined by expression (28). To first order in γ the poles are located at

$$\omega_* = \pm \omega_m - i\gamma\omega_m \quad (m = 0, 1, 2, \ldots), \tag{A1}$$

with ω_m given by expression (30). There are infinitely many poles at locations in the lower half-plane as shown in Figure 9.

The terms in the integrand in expression (27) are of the form

$$I = \int_{-\infty}^{\infty} \frac{f(\omega)}{1 + e^{i\omega\tau}e^{-\gamma|\omega|\tau}}\, d\omega, \tag{A2}$$

where $f(\omega)$ is an analytic function. Setting $\omega = \omega_* + \xi$ and using a first-order Taylor expansion in ξ gives

$$1 + e^{i\omega\tau}e^{-\gamma|\omega|\tau} = -i\xi\tau + O(\xi^2). \tag{A3}$$

This implies that the poles are simple and that the residue for the pole at ω_* is given by

$$Res\, \frac{f(\omega)}{1 + e^{i\omega\tau}} = \frac{f(\omega_*)}{-i\tau}. \tag{A4}$$

Together with the factor $-2\pi i$ from the counterclockwise contour integration, this gives a contribution $2\pi f(\omega_*)/\tau$ to the the complex integral. Using this in integral (27) and taking the poles in the third and fourth quadrant into account gives:

$$B(t) = \frac{2\pi c}{H} \sum_{m=0}^{\infty} e^{-\gamma\omega_m t} \{\cos(\omega_m(t - z/c)) + \cos(\omega_m(t - (2H - z)/c))\}. \tag{A5}$$

Using trigonometric identities the terms in curly brackets equal

$$\begin{aligned}\cos(\omega_m(t - z/c)) + \cos(\omega_m(t - (2H - z)/c)) \\ = 2\cos(\omega_m H/c)\cos(\omega_m(H - z)/c)\cos(\omega_m t) \\ - 2\sin(\omega_m H/c)\cos(\omega_m(H - z)\sin(\omega_m t).\end{aligned} \tag{A6}$$

According to expression (30), $\cos(\omega_m H/c) = 0$ and $\sin(\omega_m H/c) = (-1)^m$, so that

$$\begin{aligned}\cos(\omega_m(t - z/c)) + \cos(\omega_m(t - (2H - z)/c)) \\ = 2(-1)^{m+1}\cos(\omega_m(H - z)/c)\sin(\omega_m t).\end{aligned} \tag{A7}$$

Using this in equation (A5) gives expression (29).

Center for Wave Phenomena
Colorado School of Mines
Golden Colorado 80401
rsnieder@mines.edu
(R.S.)

U.S. Geological Survey
Pasadena, California 91106
safak@usgs.gov
(E.S.)

Manuscript received 26 May 2005.